NEW METHODOLOGY FOR SEISMIC DESIGN OF RC SHEAR WALLS

By John W. Wallace,[1] Associate Member, ASCE

ABSTRACT: An analytical approach to determine the need to provide transverse reinforcement at boundaries of reinforced concrete structural walls with rectangular, T-shaped, or barbell-shaped cross sections is presented. By relating the expected displacement demands on the building system to the local deformations imposed on the wall cross section, the magnitude and distribution of wall normal strain is determined. The primary variables affecting the wall-strain distribution are found to be the ratio of wall cross-sectional area to the floor-plan area, the wall aspect ratio and configuration, the wall axial load, and the wall-reinforcement ratios. Based on the computed wall-strain distribution, required transverse steel for concrete confinement and length of the wall cross section requiring concrete confinement is computed. The wall-strain distribution is also used to evaluate required transverse reinforcement to restrain buckling of longitudinal reinforcement. The validity of the proposed analytical approach is demonstrated by comparison with an experimental study of a full-scale building system conducted in Japan. In addition, applications of the proposed analytical approach are provided for preliminary design and for the evaluation of an existing building.

INTRODUCTION

Current U.S. code requirements [such as American Concrete Institute: ACI 318 ("Building" 1989); and *Uniform Building Code* (UBC) 1991)] for structural walls were developed with the intent of providing adequate deformability to prevent abrupt failures. To achieve deformability, well-confined boundary elements are required where the extreme fiber stress for combined gravity and earthquake loadings exceed $0.2f'_c$, where f'_c is the compressive strength of the concrete. Wall stresses are computed based on linearly elastic modeling and gross-section properties. The confinement at the wall boundary must be continued over the height of the wall until the extreme fiber stress is less than $0.15f'_c$.

A limiting wall extreme fiber stress of $0.2f'_c$ implies that earthquake forces five times the code specified forces could be resisted by the wall prior to significant inelastic response. However, given current UBC force-reduction factors of six and eight for bearing- and shear-wall buildings, respectively, current codes assume very little inherent deformability for structural wall buildings (where structural walls are constructed without special transverse reinforcement for concrete confinement) and, by inference, relatively little wall-deformation capacity.

A significant shortcoming of approaches that assume a single implicit force-reduction factor for structural-wall buildings is that a conservative value must be selected for a given building configuration (e.g., shear wall buildings); therefore, a majority of buildings are likely to be overdesigned. Given this limitation, the system ductility factor may not be closely related to the expected behavior of the system, but instead provides a somewhat arbitrary set of lateral forces for determining required details. Research by

[1]Asst. Prof., Dept. of Civ. and Envir. Engrg., Box 5710, Clarkson Univ., Potsdam, NY 13699-5710.

Note. Discussion open until August 1, 1994. To extend the closing date one month, a written request must be filed with the ASCE Manager of Journals. The manuscript for this paper was submitted for review and possible publication on July 2, 1992. This paper is part of the ***Journal of Structural Engineering***, Vol. 120, No. 3, March, 1994. ©ASCE, ISSN 0733-9445/94/0003-0863/$2.00 + $.25 per page. Paper No. 4323.

Wallace and Moehle (1992) has shown that current code requirements are overly conservative for a vast majority of building systems utilizing structural walls for lateral load resistance. Instead of a single system ductility factor, Wallace and Moehle (1992) presented a displacement-based approach that relates the need to provide concrete confinement at wall boundaries to the expected building response. The primary variables affecting wall details were found to be the ratio of wall cross-sectional area to floor-plan area, the wall aspect ratio and configuration, the wall axial load, and the wall-reinforcement ratios. Therefore, wall details are tied intrinsically to the building configuration, and changes in building configuration lead to changes in required details (transverse reinforcement).

OBJECTIVES AND SCOPE

Current U.S. (and foreign) code requirements for confinement of structural walls do not properly discern those cases in which concrete confinement is required or not required, and are generally quite conservative. Therefore, there is a need to establish new guidelines for the proportion and detail of structural walls. The guidelines should be applicable to all regions of the U.S. and to structural walls with various cross sections. The studies reported herein focus on presenting a methodology for developing new code provisions for seismic design of reinforced concrete shear walls by modifying and expanding the displacement-based approach presented by Wallace and Moehle (1992).

DISPLACEMENT-BASED APPROACH: OVERVIEW

Unlike current code procedures, which are strength based, a displacement approach compares directly the expected displacement capacities and displacement demands for the building. Therefore, reinforcing details are directly related to expected building response. The overall process can be summarized as follows:

1. Ensure minimum level of building strength
2. Characterize earthquake demands at building site
3. Characterize global (building) deformations
4. Characterize local (structural element) deformation capacity
5. Relate global and local deformations
6. Establish detailing requirements

The following sections describe the details of the displacement-based approach for structural wall systems in regions of high seismic risk. Characterization of the earthquake ground motions and global building deformations are discussed in the first section, followed by a section that discusses estimates of local deformation capacity of a wall cross section. The third section focuses on relating global and local deformations, whereas the final section investigates detailing requirements.

CHARACTERIZATION OF EARTHQUAKE GROUND MOTIONS

Studies reported by Newmark and Hall (1982) and Shimazaki and Sozen (1984) examine the maximum inelastic and elastic displacement responses of single-degree-of-freedom oscillators. These studies find that if the initial period exceeds the characteristic ground period (approximately the period

at which the constant acceleration and constant velocity regions coincide, or approximately 0.5 s for firm soil sites) the maximum displacement is nearly independent of strength. If the initial period is less than the characteristic ground period, inelastic displacements are expected to be larger than the elastic displacements. Newmark and Hall (1982) present an approach to develop an inelastic displacement spectrum from the elastic displacement spectrum; therefore, elastic displacement spectra are suitable tools for estimating maximum displacement response.

Displacement response spectra can be developed for a particular building site, or generalized spectra such as those presented in Applied Technology Council's ATC-3-06 ("Tentative" 1978) can be used. In the present paper, a generalized spectrum will be used to present the fundamentals of the displacement based approach. According to ATC-3-06, spectral acceleration for elastic response is

$$S_a = \frac{1.2A_vS}{T^{2/3}} \quad \ldots\ldots (1)$$

except S_a need not exceed 1.0 for soil types 1 ($S = 1.0$) and 2 ($S = 1.2$), and need not exceed 0.8 for soil type 3 ($S = 1.5$). (It is noted that subsequently a fourth soil condition was added to ATC-03-06.) In (1), T is the fundamental period of vibration of the structural system (in the direction under consideration); S is a factor to account for soil characteristics; and A_v is a factor to account for seismicity. The two-thirds exponent was included in (1) as a safety factor for taller buildings and longer period structures for which higher modes may significantly influence internal forces. Since displacements are not likely to be influenced significantly by higher modes, and because the approach being developed is based on displacements, the two-thirds exponent is dropped. With the modified exponent, the elastic spectral displacement can be computed in terms of the elastic spectral acceleration as

$$S_d = \frac{T^2S_a}{4\pi^2} = \frac{1.2A_vST}{4\pi^2} \quad \ldots\ldots (2)$$

Assuming values $A_v = 0.4$ and $S = 1.2$ (for firm soil sites), an expression for elastic spectral displacement is obtained from Eq. (1) and (2) as follows:

$$S_d = 10T^2 \text{ (in.)} \quad 0.0 \le T \le 0.585 \text{ s} \quad \ldots\ldots (3a)$$

$$S_d = 6T \text{ (in.)} \quad 0.585 \text{ s} < T \quad \ldots\ldots (3b)$$

$$S_d = 25T^2 \text{ (cm)} \quad 0.0 \le T \le 0.585 \text{ s} \quad \ldots\ldots (3c)$$

$$S_d = 15T \text{ (cm)} \quad 0.585 \text{ s} < T \quad \ldots\ldots (3d)$$

The period range for which (3*a*) and (3*c*) are applicable represents a region of constant acceleration, whereas (3*b*) and (3*d*) represent a region of constant velocity. The elastic displacement response spectrum as given by (3) may be considered representative of 5% damped spectra for strong ground motions on firm soil in the United States. Eqs. (3*a*) and (3*b*) are plotted in Fig. 1.

The relationships plotted in Fig. 1 can be modified to incorporate the effects of inelastic response based on the procedure presented by Newmark and Hall (1982). It is noted that other procedures are available such as that proposed by Qi and Moehle (1991). The procedure derives inelastic accel-

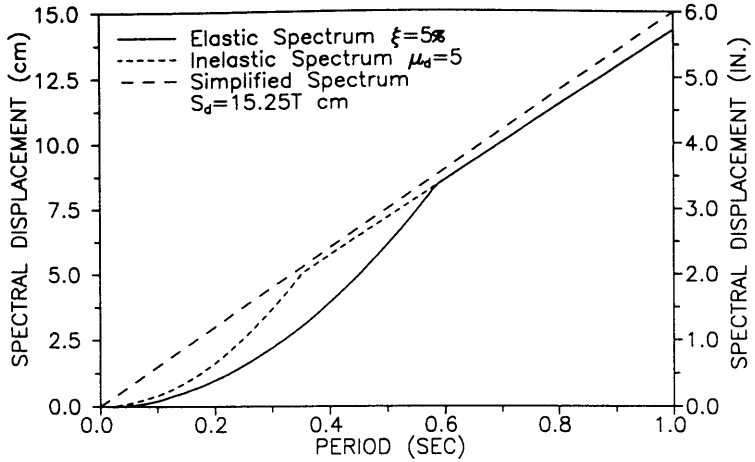

FIG. 1. Elastic and Inelastic Displacement Spectra

eration and displacement spectra from the elastic spectrum given a displacement ductility factor. Fig. 1 also includes an inelastic displacement spectra for a displacement ductility ratio of five, and a simplified spectrum [S_d = 15T cm (6T in.)]. Fig. 1 reveals that the linear spectrum [S_d = 15T cm (6T in.)] gives an envelope of the inelastic spectra; therefore, the linear spectrum may be used to provide an estimate of the maximum elastic and inelastic displacement for all periods (the estimate will tend to be conservative for periods less than approximately 0.3 s). A linear spectrum [S_d = 15T cm (6T in.)] is used in all subsequent calculations for spectral displacement.

ESTIMATING GLOBAL BUILDING RESPONSES

Estimates of building displacement can be obtained from a displacement spectrum given an estimate of the fundamental period. For structural wall buildings, the fundamental period based on a cracked section stiffness can be estimated as (Wallace and Moehle 1992)

$$T = 8.8 \frac{h_w}{l_w} n \sqrt{\frac{wh_s}{gE_c p}} \quad \ldots\ldots (4)$$

in which n = number of floors; w = unit floor weight including tributary wall height; h_s = mean story height; E_c = concrete modulus of elasticity; h_w = wall height; and p = ratio of wall area to floor plan area for the walls aligned in the direction the period is calculated ($p = \Sigma A_w/A_f$, where $A_w = l_w t_w$, l_w is the wall length, t_w is the wall thickness, and A_f is the floor plan area of a typical floor of the building). Eq. (4) assumes all walls have the same cross section (the equation can be modified to account for walls with different cross sections). The validity of (4) was verified by comparison with measured periods for shear wall buildings (Wallace and Moehle 1992; Yan and Wallace 1993).

For a shear wall building, roof displacement can be approximated by 1.5 times the spectral displacement (to account for the difference between the displacement of a single-degree-of-freedom oscillator and the building system the oscillator represents). Therefore, the roof drift (roof displacement

divided by building height, δ_u/h_w) can be computed by multiplying (3b) or (3d) by 1.5 and dividing by the building (wall) height, h_w.

$$\frac{\delta_u}{h_w} = \frac{1.5(S_d)}{h_w} \quad \ldots\ldots (5)$$

The roof drift can be expressed in terms of the wall aspect ratio and the ratio of wall area to floor plan area by substituting the period T as given by (4) for T in (3), and substituting the result into (5)

$$\frac{\delta_u}{h_w} = 80 \frac{h_w}{l_w} \sqrt{\frac{w}{gE_c p h_s}} \quad \ldots\ldots (6)$$

For typical values of w = 8.4 kPa (175 psf), h_s = 275 cm (108 in.), g = 981 cm/s^2 (386.4 in./s^2), and E_c = 24,000 MPa (3,500 ksi), (6) can be expressed as

$$\frac{\delta_u}{h_w} = 0.00023 \frac{h_w}{l_w} \sqrt{\frac{1}{p}} \quad \ldots\ldots (7)$$

which is plotted in Fig. 2 for several wall aspect ratios and is valid for elastic or inelastic response. The roof drift ratio obtained should tend to be conservative because the period T given by (4) is based on half the gross-section stiffness (and the "typical" values are selected to produce a high drift estimate).

The roof drift ratio provides an estimate of the global deformation demands on the building. The global deformations of the structure are related to local deformations imposed on the wall cross section in the following section.

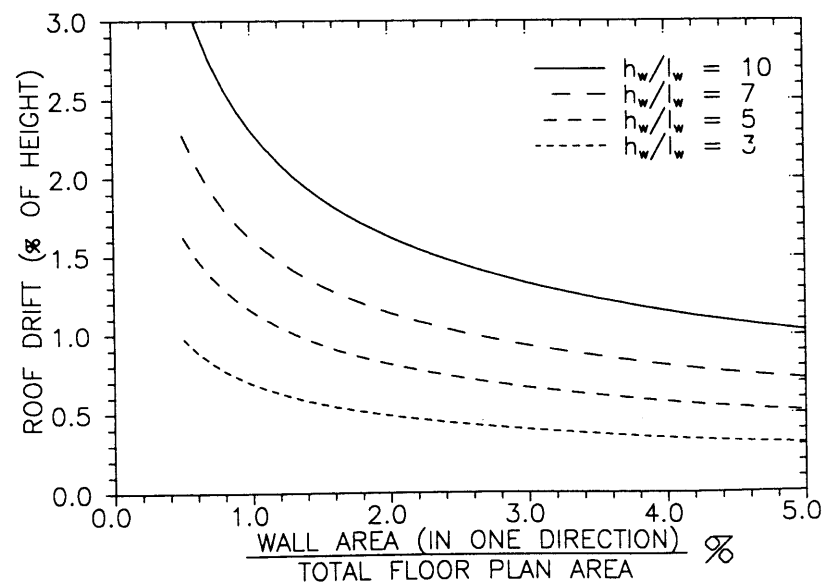

FIG. 2. Estimate of Roof Drift Ratio

RELATING GLOBAL AND LOCAL DEFORMATIONS

The deformation imposed on individual walls as a result of the global building deformations can be evaluated using well-established procedures to account for the distribution of elastic and inelastic deformations over the wall height. Based on the model of Fig. 3, the displacement at the top of the wall can be computed as

$$\delta_u = \delta_y + \theta_p h_w = \frac{11}{40}\phi_y h_w^2 + \frac{1}{2}(\phi_u - \phi_y) h_w l_w \quad \ldots\ldots (8)$$

where δ_y = displacement resulting from elastic deformations; $\theta_p h_w$ = displacement resulting from inelastic deformations; h_w = wall height; l_w = wall length; ϕ_y = yield curvature (curvature at first yield of the wall boundary reinforcement); ϕ_u = ultimate curvature; and l_p and θ_p = plastic hinge length and rotation, respectively. Based on this relation and assumptions for yield curvature ($0.0025/l_w$) and plastic hinge length ($0.5l_w$), the deformations imposed on a wall can be derived in terms of the ultimate curvature times the wall length (Wallace and Moehle 1992).

$$\phi_u l_w = 0.0025\left[1 - \frac{1}{2}\frac{h_w}{l_w}\right] + 2\frac{\delta_u}{h_w} \quad \ldots\ldots (9)$$

If (7) is substituted in (9), the deformation imposed at the base of the wall can be expressed directly in terms of the building configuration as

$$\phi_u l_w = 0.0025\left[1 - \frac{1}{2}\frac{h_w}{l_w}\right] + 0.00046\frac{h_w}{l_w}\sqrt{\frac{1}{p}} \quad \ldots\ldots (10)$$

Eq. (10) describes the deformation (ultimate curvature) imposed on the wall cross section. The need to provide concrete confinement can be evaluated by comparing directly the deformations imposed on the wall cross section with the available deformation capacity of the wall cross section. Wall deformation capacity is estimated in the following section.

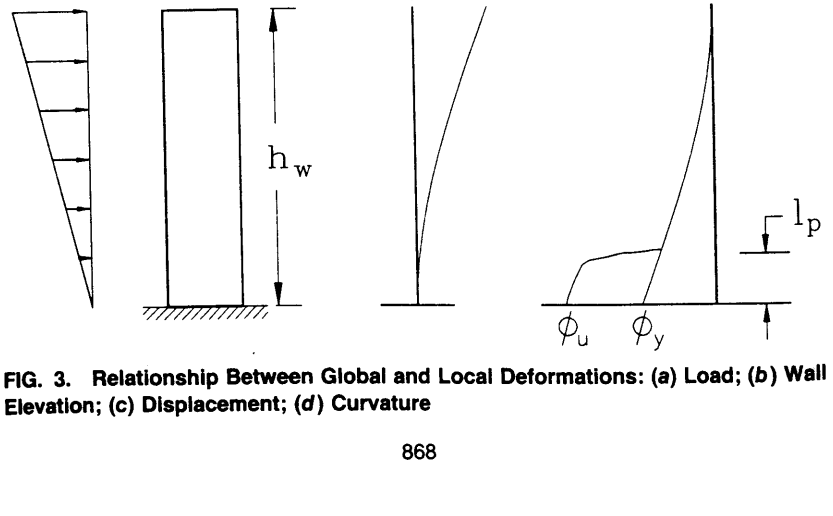

FIG. 3. Relationship Between Global and Local Deformations: (*a*) Load; (*b*) Wall Elevation; (c) Displacement; (*d*) Curvature

ESTIMATING WALL-DEFORMATION CAPACITY

The deformation capacity of a wall cross section can be estimated using the model of Figs. 4 and 5. The wall has uniformly distributed reinforcement plus boundary steel. Axial load is centered on the wall web. The longitudinal tension and compression reinforcement is assumed to develop a stress of αf_y and γf_y, respectively, to account for possible material overstrength and strain hardening ($\alpha = 1.50$ and $\gamma = 1.25$ are used in the subsequent analyses). Based on equilibrium of the wall cross section, the following relations can be derived for rectangular, T- and L-shaped walls [(11) and Fig. 4] and barbell-shaped walls [(12) and Fig. 5]

$$\varepsilon_{c,\max} = \left[\frac{\left(\rho + \rho'' - \frac{\gamma}{\alpha}\rho'\right)\frac{\alpha f_y}{f_c'} + \frac{P}{l_w t_w f_c'}}{\left(0.85\beta_1 + 2\rho''\frac{\alpha f_y}{f_c'}\right)}\right]\phi_u l_w \quad \ldots\ldots (11)$$

$$\varepsilon_{c,\max} = \left[\frac{\left(\rho + \rho''\right)\frac{\alpha f_y}{f_c'} - \rho'\frac{\gamma f_s'}{f_c'} - \frac{0.85b}{t_w l_w}\left(a - t_w\right) + \frac{P}{l_w t_w f_c'}}{\left(0.85\beta_1 + 2\rho''\frac{\alpha f_y}{f_c'}\right)}\right]\phi_u l_w$$

$\ldots\ldots (12)$

where $\varepsilon_{c,\max}$ = extreme fiber concrete strain; $\rho = A_s/t_w l_w$ is the tension

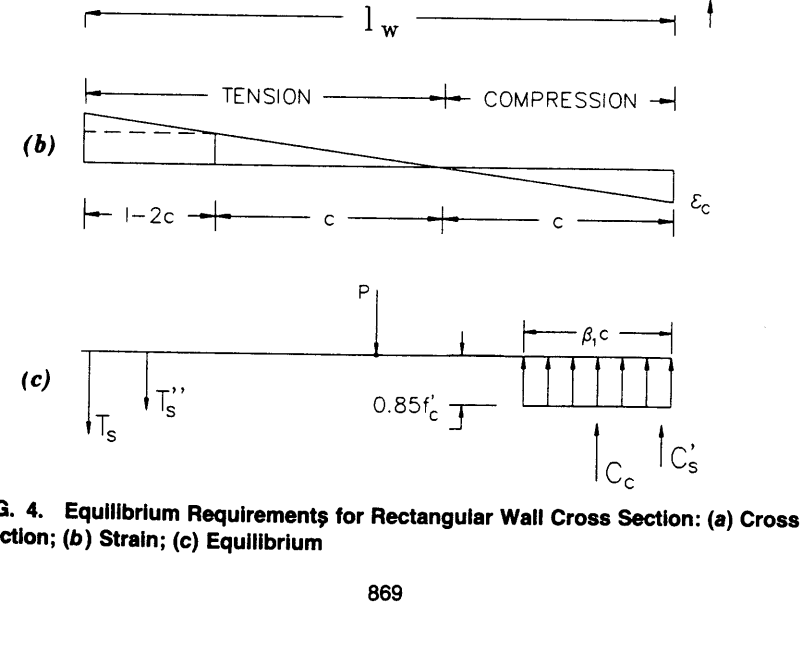

FIG. 4. Equilibrium Requirements for Rectangular Wall Cross Section: (*a*) Cross Section; (*b*) Strain; (*c*) Equilibrium

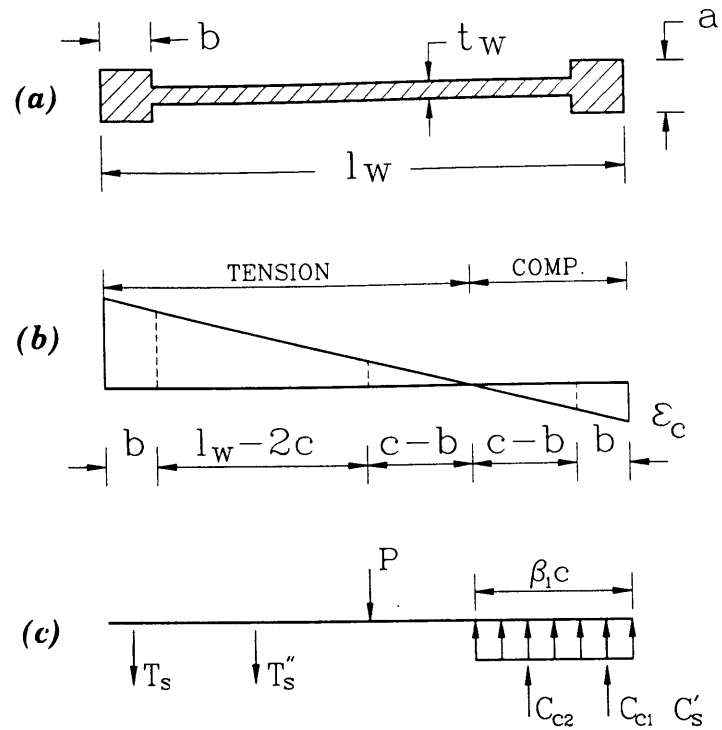

FIG. 5. Equilibrium Requirements for Barbell-Shaped Wall Cross Section: (*a*) Cross Section; (*b*) Strain Distribution; (*c*) Equilibrium

steel reinforcing ratio; $\rho' = A_s'/t_w l_w$ is the compression steel reinforcing ratio; $\rho'' = A_s''/t_w l_w$ is the distributed steel reinforcing ratio; β_1 is a factor defined in ACI 318-89 section 10.2.7.3 ("Building" 1989); P = axial load; f_y = nominal yield stress of the steel; f_s' = stress in the compression steel; t_w = web thickness; b = length of the boundary element; and a = thickness of the boundary element (Fig. 5). For T- and L-shaped walls, the maximum extreme fiber compression strain arises when the flange of the T- or L-shaped section is in tension; therefore, an effective flange width must be determined. Paulay (1986) suggests an approximate approach to estimate the effective flange width (for slender walls, the entire flange is typically effective). All reinforcement within the effective flange width should be included in calculating the tension reinforcing ratio ρ. For (12), the neutral axis is assumed to be within the wall web. The stress in the compression reinforcement can be assumed to be at yield; however, this should be verified. A similar expression can be derived for the neutral axis within the boundary element and an iterative approach should be used to verify the stress in the compression reinforcement and to converge to a unique solution. It should also be noted that (11) and (12) are valid only where the depth of the neutral axis is not greater than one-half the wall length l_w.

Eqs. (11) and (12) can be used directly with (10) to determine the maximum compressive strain that will develop at the wall boundary. At first glance, the equations appear to be too detailed for design; however, all

terms in the equations are readily available and no detailed analysis or design is required. In addition, for symmetrically reinforced walls, the equations can be simplified. Application of the equations to preliminary design and in the evaluation of existing construction are discussed later in the present paper.

The need to provide concrete confinement at the wall boundary can be established by examining the maximum concrete strain and the distribution of concrete strain along the wall cross section. This topic is considered in the next section.

DETAILING REQUIREMENTS

The need to provide concrete confinement at the boundaries of structural walls can be evaluated by substituting (10) into (11) or (12). The equations indicate that the maximum concrete compressive strain for a structural wall depends on general response quantities (the ground motion characteristics at the building site and the fundamental period of the building) and the building and wall attributes (wall reinforcing ratios, wall axial stress, material properties, wall aspect ratio, and ratio of wall area to floor-plan area).

Maximum Concrete Compression Strain

Fig. 6 plots the computed extreme fiber compression strain for symmetrically reinforced walls (for $f_c' = 27.5$ MPa (4,000 psi), $f_y = 413$ MPa (60 ksi), $\rho = \rho' = 0.01$, $\rho'' = 0.0025$), and reveals that extreme fiber compression strain: (1) Increases with the level of axial stress [Fig. 6(*a*)]; (2) increases in wall aspect ratio [Fig. 6(*b*)]; and (3) decreases with as the ratio of wall area to floor plan area increases [Fig. 6(*a* and *b*). Fig. 6 provides a convenient means of evaluating the need to provide transverse reinforcement for concrete confinement. For example, given an axial load of $P = 0.10A_w f_c'$, Fig. 6(*a*) [or 6(*b*)] reveals that where the ratio of wall area to floor area in one direction of the building exceeds 0.01 and the wall aspect ratio is less than five, the extreme fiber compression strain is 0.0045 or less. Since structural elements are capable of extreme fiber compression strains of 0.004 without significant detrioration in strength, the analysis indicates that there is a large class of buildings for which special detailing at the wall boundaries is not required.

Fig. 7 plots computed extreme fiber strain for unsymmetrically reinforced wall cross sections for $h_w/l_w = 5$ and $P = 0.10A_w f_c'$ (for $f_c' = 27.5$ MPa (4,000 psi), $f_y = 413$ MPa (60 ksi), $\rho = 0.01$ to 0.02, $\rho' = 0.01$, and $\rho'' = 0.0025$). (For example, a T-shaped wall where all of the flange reinforcement is assumed to be effective as tension reinforcement; therefore, ρ exceeds ρ'.) Fig. 7 indicates that the computed extreme fiber compression strain increases as the difference in the tension and compression steel reinforcing ratios increase. Therefore, design of walls with T- or L-shaped cross sections are more likely to require special transverse reinforcement for concrete confinement and to suppress bucking of the longitudinal reinforcement (in the stem of the wall).

U.S. code formats generally result in the use of relatively few shear walls; therefore, ratios of wall area to floor plan area of 0.5–1.0% are common. From a review of Figs. 6 and 7, it is apparent that the ratio of wall area to floor plan area plays a major role in the expected performance of shear wall buildings. At ratios less than 1%, Figs. 6 and 7 indicate a substantial increase in extreme fiber compression strain. In addition, where relatively few walls

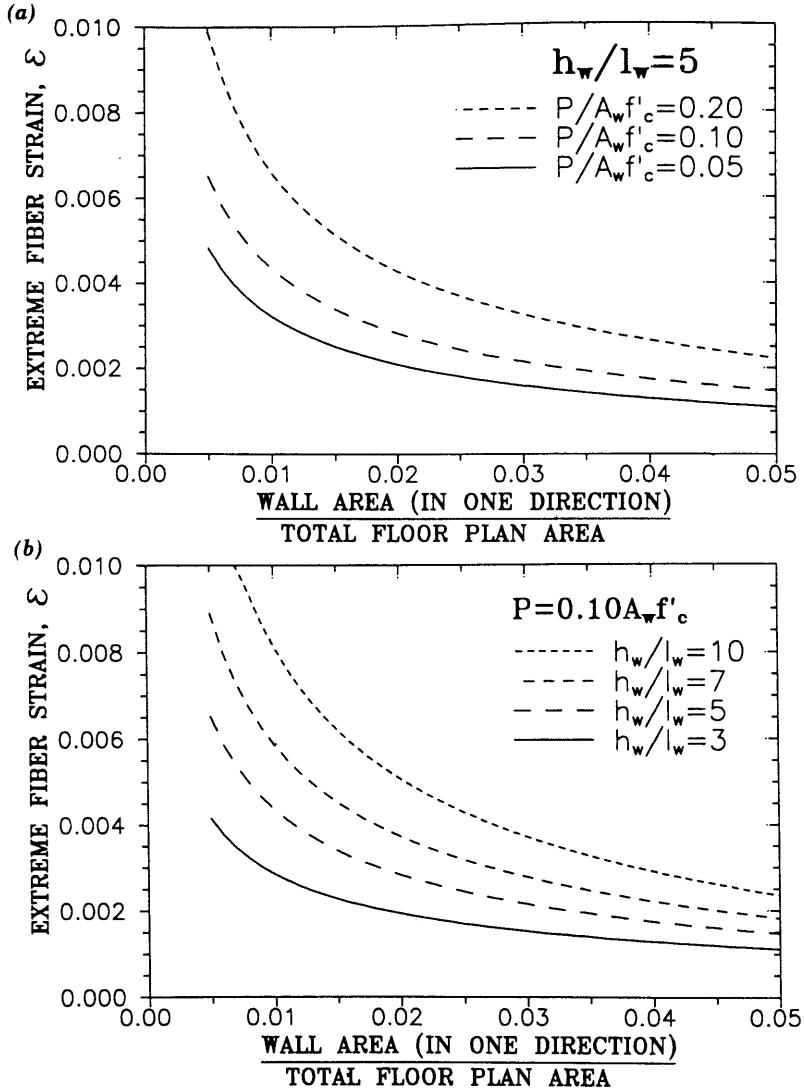

FIG. 6. Computed Wall Extreme Fiber Strain: (*a*) for Constant Aspect Ratio; (*b*) for Constant Axial Load

are used to resist lateral loads, damage to one of the walls could potentially result in significant torsional effects; therefore, well confined boundary elements are necessary to ensure adequate behavior. Conversely, Figs. 6 and 7 indicate a substantial reduction in extreme fiber compression strain as the ratio of wall area to floor plan area is increased from 0.5 to 1.5%; therefore, as an alternative to U.S. design tendencies, construction utilizing a greater number of walls might allow for greater design flexibility by alleviating the need for well confined boundary elements.

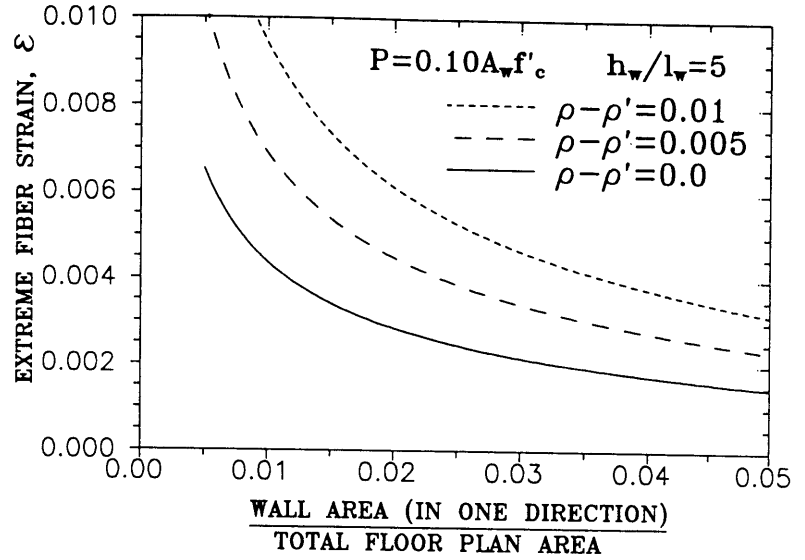

FIG. 7. Computed Wall Extreme Fiber Strain for Unsymmetrically Reinforced Walls

Required Zone of Confinement

The depth of the wall cross section that requires confinement can be determined from (11) [or (12) for barbell-shaped walls] if it is noted that $\varepsilon_{c,max} = c\phi_u$, where c is the depth of the compression zone. The resulting equation gives the depth of the compression zone as a function of the wall length (l_w). Given the extreme fiber compressive strain and the depth of the compression zone, the portion of the wall cross section requiring confinement can be estimated if it is assumed that concrete confinement should be provided at locations where the concrete compressive strain exceeds a limiting value, for example 0.004.

Figs. 8 and 9 plot the required length of confinement for a limiting compression strain of 0.004 for symmetrically (Fig. 8) and unsymmetrically (Fig. 9) reinforced walls with rectangular, T- and L-shaped cross sections (for f'_c = 27.5 MPa (4,000 psi), f_y = 413 MPa (60 ksi), ρ'' = 0.0025). Figs. 8 and 9 provide a direct approach to determine the required depth of confinement for the wall cross section, and also reveal that concrete confinement is unlikely for symmetrically reinforced walls with low to moderate levels of axial stress. For walls that require concrete confinement, the amount of transverse steel required depends on the level of concrete compressive strains (due to space limitations, this topic is not covered in the present paper).

Transverse Steel Spacing Requirements for Buckling

The amount of transverse steel required at the critical portion of a wall cross section depends not only on the need to confine the concrete, but also on the tendency of the longitudinal reinforcing steel to buckle. The tangent modulus theory [see Salmon and Johnson (1990) for a review of buckling models] can be used to estimate the required spacing of transverse steel to prevent buckling of compression steel. Research on buckling (Mau 1990) indicates that use of the tangent modulus theory (with an end restraint coefficient provided by the transverse steel of 0.5) is appropriate for trans-

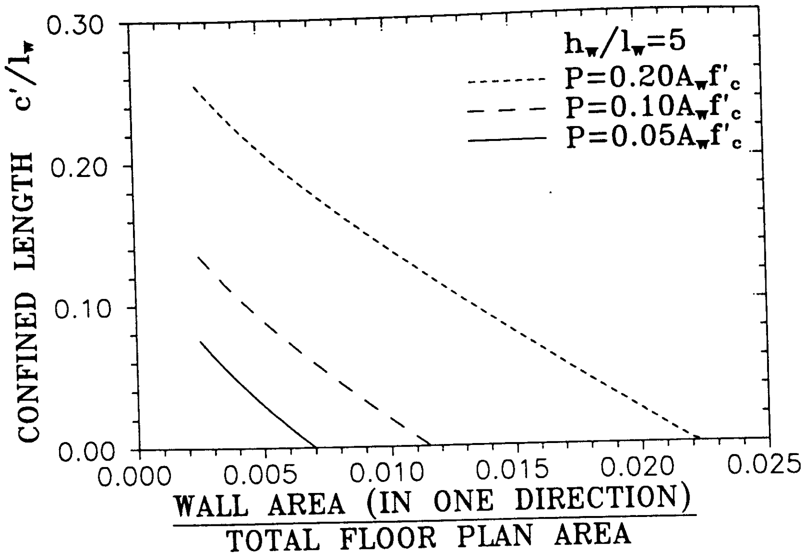

FIG. 8. Required Wall Length for Concrete Confinement for Constant Aspect Ratio

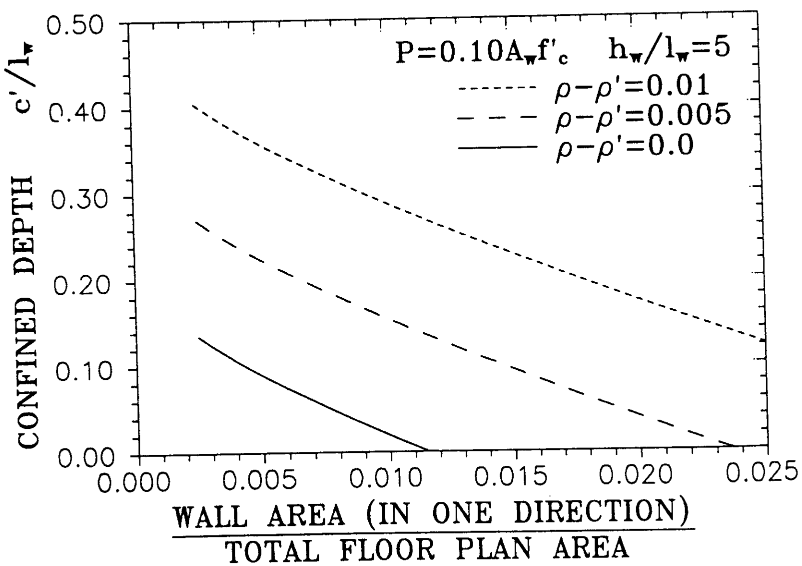

FIG. 9. Required Wall Length for Concrete Confinement for Unsymmetrically Reinforced Walls

verse spacing-to-longitudinal reinforcing bar diameters expected at wall boundaries. Therefore, a restraint coefficient of 0.5 is used in the present paper and results in the following:

$$s_{max} = 1.6d_b\sqrt{\frac{E_t}{f_s}} \quad \text{(13)}$$

where s_{max} = maximum spacing of the transverse steel to suppress buckling of the longitudinal reinforcing steel; d_b = reinforcing bar diameter; E_t = tangent modulus of the reinforcing steel; and f_s = reinforcing bar stress. Based on (13), required spacing can be estimated for a given level of compressive strain (and an assumed steel stress-strain relationship). Therefore, the quantity of transverse steel required to both confine the concrete and restrain buckling of the reinforcing steel can be evaluated in terms of the strain distributions described by (10) and (11) for walls with rectangular, T- and L-shaped cross sections, and (10) and (12) for walls with barbell-shaped cross sections. Use of (10)–(12) should allow for increased design flexibility because they enable the designer to evaluate minimum spacing requirements based on the expected building performance (wall deformations), whereas current code provisions are indiscriminate.

FRAME-WALL INTERACTION AND COUPLED WALLS

The derivations and conclusions in the previous sections are based on the lateral response of cantilever walls; therefore, the results are readily applicable to bearing wall buildings in which walls are coupled by slabs and for buildings with "light" perimeter frames. However, for other wall buildings, frame-wall interaction will affect demands on the walls and thus wall detailing requirements. Consideration of the effects of frame-wall interaction and coupled walls are discussed in the following paragraphs.

Frame-wall interaction generally results in reduced lateral displacements at upper floors and affects the distribution of wall moment over the height of the building (reversed curvature may occur in the upper floors). The equations presented for cantilever walls could be modified to consider the effects of frame-wall interaction on displacement and curvature distribution (for example, a multiplier of 1.3 could be used to determine roof drift from the spectral displacement); however, this would result in undue complication. Because the frame-wall interaction will result in a reduction of roof drift, it is reasonable to neglect the interaction in estimating roof drift (and period). In addition, the effect of frame-wall interaction on the wall curvature distribution can also be neglected since changes in elastic curvature distribution in upper stories are of minor consequence (to be conservative, all of the deformation required to achieve the roof displacement could be assumed to be inelastic rotation over the plastic hinge length at the base of the wall). To ensure that the plastic hinge occurs at the base of the wall a strength envelope over the wall height such as that recommended by Paulay (1986) could be used.

As noted in Figs. 6(*a*) and 8, greater levels of axial stress increase the likelihood that special transverse reinforcement will be required (as would be expected). For coupled walls, the level of axial load on the wall increases (on either wall due to load reversals) because the wall must resist the shear forces that act at the end of the coupling beams that frame into the wall (in addition to the tributary gravity loads). To estimate the level of axial stress for coupled walls, all coupling beams that frame into the wall can be assumed to be in reverse curvature with ultimate (plastic) moments at the ends of the coupling beams (Fig. 10).

DESIGN FOR SHEAR

For bearing-wall buildings, the ratio of wall area to floor-plan area is usually sufficient to preclude wall shear failure modes. However, frame-

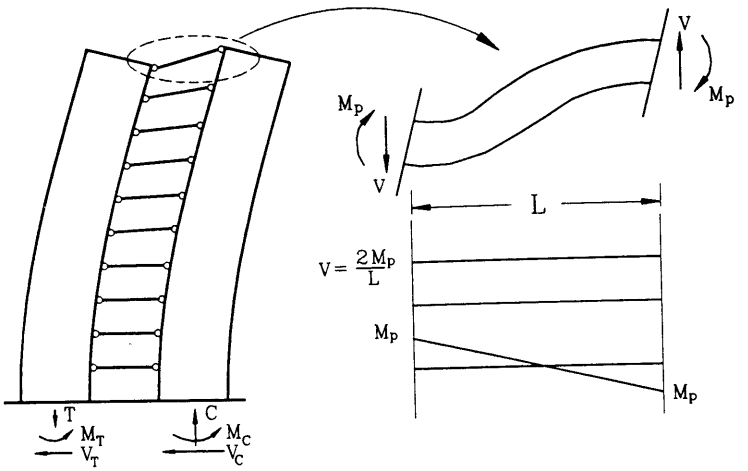

FIG. 10. Influence of Coupling Beams on Wall Axial Load

wall interaction results in an increase in the slope of the moment diagram over the lower levels of the wall, and thus increases the level of shear stress that must be resisted by the wall compared with cantilever walls. In addition, for walls with coupling beams, a greater portion of the lateral shear is resisted by the wall with increased axial load. Therefore, greater attention to design for shear is required for frame-wall and coupled wall systems compared to bearing-wall systems. Additional research is needed to address the effects of shear on frame-wall systems constructed with rectangular walls. However, until additional information is available, a reduced level of maximum design shear stress is recommended. For example, a maximum shear stress of $6\sqrt{f'_c}$ as recommended by Aktan and Bertero (1985) could be used compared with current UBC-91 (*Uniform* 1991) values of $8\sqrt{f'_c}$ for all walls sharing a common lateral force and $10\sqrt{f'_c}$ for an individual wall.

BUILDING APPLICATIONS

To detail the potential uses of the analytical approach presented, three applications are presented. The first application compares analytical and experimental results for a full-scale building tested in Japan (Hirosawa et al. 1981). The second application involves the use of the proposed approach for preliminary design, followed by an application to an existing building where findings are compared with results obtained using current code approaches. The applications are detailed in the following sections.

Application 1: Full-Scale Test of Bearing-Wall Building

The test specimen consisted of a three-bay, full-scale model of the bottom five stories of an eight-story reinforced concrete (RC) wall building (Fig. 11). The test specimen consisted of four planes (Y_0, Y_1, Y_2, and Y_3) with various wall cross sections. The planes were constructed to include beams with nonstructural walls (plane Y_0), walls with openings (planes Y_1 and Y_3), walls with finish materials (plane Y_1), and walls with openings and doors (plane Y_2). The walls were coupled in-plane with beams.

Reinforcing details for plane Y_2 are provided in Hirosawa et al. (1981).

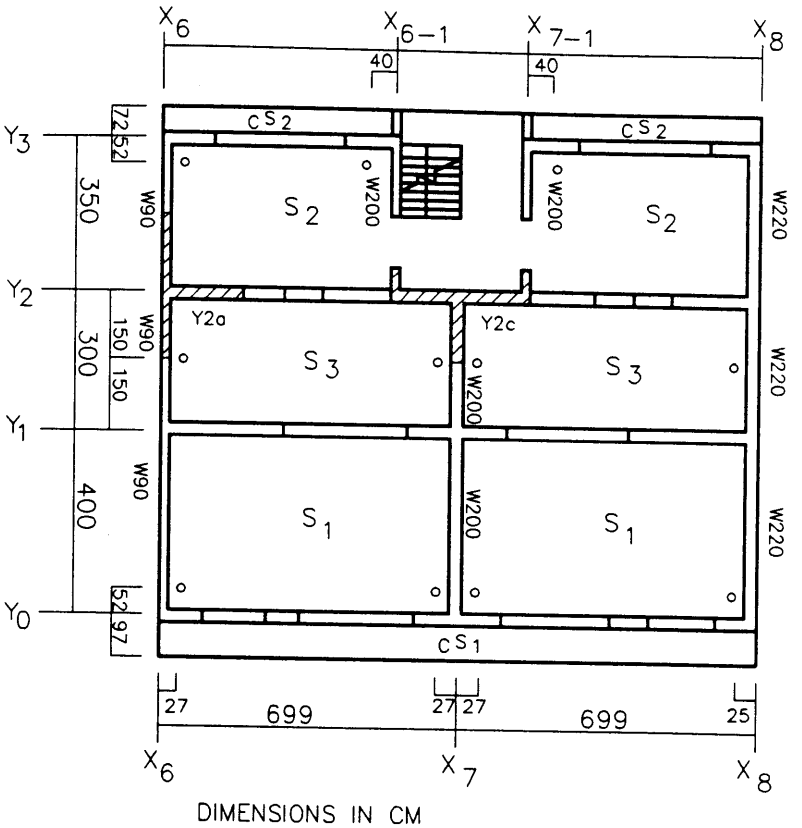

FIG. 11. Plan View of Full-Scale Bearing Wall Test Structure

Additional reinforcing details were obtained directly from the Building Research Institute (BRI). The walls were 27 cm (10.63 in.) for stories one and two, and 25 cm (9.84 in.) for the remaining stories. Reinforcing bar sizes used at the wall boundaries varied from No. 25 mm bars (approximately No. 8 U.S. bar) to No. 13 mm bars (approximately No. 4 U.S. bar). Vertical web steel consisted of 13 mm bars at 20 cm (approximately No. 4 U.S. bar at 7.87 in.).

Material properties are based on average values obtained from BRI test results: Concrete properties were f'_c = 25 MPa (3.6 ksi) and E_c = 23,000 MPa (3,300 ksi); Steel properties were f_y = 377 MPa (54 ksi) and f_u = 560 MPa (81 ksi). A story height of 265 cm (104.3 in.) was used for a total eight-story building height of 21.2 m (69.5 ft). An axial load of 8.4 MN (1,890 kips) was applied using hydraulic actuators to simulate the vertical loading of stories six through eight and the total building weight was 18.7 MN (4,200 kips). The test specimen was subjected to reversed cyclic drift to simulate earthquake loading (the loads were applied to result in a wall base moment equivalent to the eight-story structure subjected to a uniform load over the building height).

Because walls of various geometries were used, an effective ratio of wall area to floor plan area and an effective wall aspect ratio were computed to

determine a fundamental period and to estimate roof displacement for the design earthquake ground motions as follows:

$$I_{\text{total}} = \sum_{i=1}^{n} \frac{t_{wi} l_{wi}^3}{12} \quad \ldots\ldots (14)$$

$$l_{w,eff} = \left[\frac{12 I_{\text{total}}}{n \bar{t}_w} \right]^{1/3} \quad \ldots\ldots (15)$$

$$P_{eff} = \frac{n \bar{t}_w l_{w,eff}}{A_f} \quad \ldots\ldots (16)$$

where t_{wi} = thickness of the ith wall; l_{wi} = length of the ith wall; and $\bar{t}_w$ = average wall thickness. The effective ratio of wall area to floor plan area p_{eff} for the eight-story building is 0.0384, resulting in a period estimate 1.5 s based on using (4) with h_w = 2,120 cm, l_w = 180 cm, and w = 10.8 kPa. A simplified linear spectrum is used to obtain an estimate of roof drift for a damageability limit state based on (6), and results in a maximum lateral roof drift of 1.6%.

Load-deformation relations reported by Hirosawa et al. (1981) indicate the maximum lateral load of approximately 90% of the building weight was obtained at a roof drift ratio of 1%; however, a roof drift ratio of 2% was achieved without significant deterioration in lateral load capacity. Therefore, the experimental results indicated adequate load-deformation capacity for the damageability limit state.

Detailed damage patterns were provided for axis Y_2 at 0.125%, 0.25%, 0.5%, 1%, and 2% lateral drift (Hirosawa et al. 1981). Significant base wall diagonal and flexural cracking was noted at 0.25% drift. Damage for subsequent cycles (0.5 and 1%) consisted of the extension of existing cracks and additional diagonal and flexural cracks in upper stories. Significant damage was noted at 2% lateral drift, and was concentrated in high aspect ratio walls in levels four and five (apparently due to a "weak column" condition as the beams at floors three and four were "beefed up" to account for the coupling effects of floors six through eight), and at the base of the walls. Crushing at the wall boundary was indicated at 2% lateral drift for one wall along axis Y_2 (evaluated in the following paragraph as wall Y_{2c}).

Two walls of the BRI building, Walls Y_{2a} and Y_{2c} (Fig. 11), are evaluated to determine whether adequate wall deformation capacity is predicted with the proposed analytical approach. The wall cross sections are 27 × 189 cm (10.63 in. × 74.4 in.) for Y_{2a} and 27 cm × 300 cm (10.63 in. × 118.1 in.) for Y_{2c}. Aspect ratios for the two walls evaluated are 11.2 (Y_{2a}) and 7.1 (Y_{2c}) for the eight-story prototype structure. Axial load on the walls was estimated based on tributary areas to be $0.065 A_w f'_c$ and $0.05 A_w f'_c$ for walls Y_{2a} and Y_{2c}, respectively. Based on the reinforcing details and wall geometry given in Fig. 12 (Hirosawa et al. 1981), the wall drift capacity was computed using (10) and (11) assuming a limiting concrete extreme fiber compression strain of 0.004 (for higher strains, it is expected that crushing at the wall boundary would be noticeable). The analytical results indicate drift capacities of approximately 1.6% for both walls. The analytical evaluation is consistent with the test results (which revealed a drift capacity of 1% for maximum lateral strength and 2% prior to significant wall damage). Comparison with a damageability limit state based on a displacement spectrum of 15T cm (6T in.) (1.6% roof drift in the design earthquake) suggests that

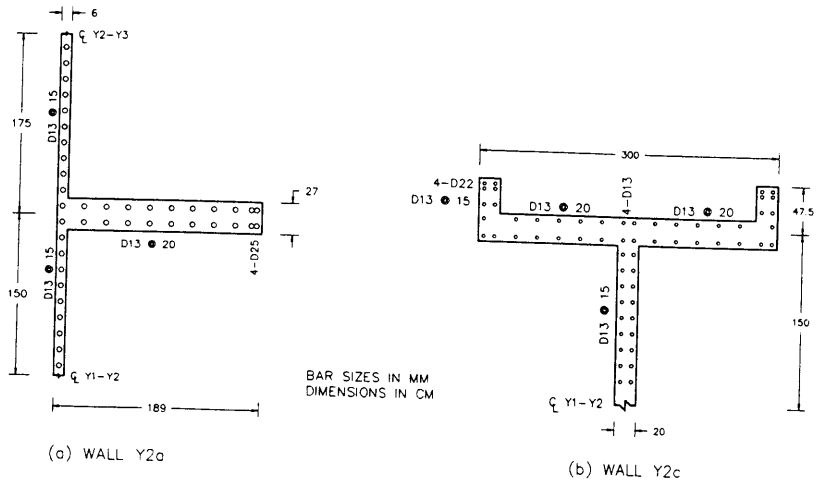

FIG. 12. Wall Geometry and Reinforcing Details for BRI Test Structure

transverse reinforcement for concrete confinement is not required at the wall boundaries, and is consistent with the experimental results.

Application 2: Preliminary Design

The proposed analytical approach can easily be applied to assist in preliminary design. For example, consider a five-story building with floor plan dimensions of 30.5 × 15.25 m (100 × 50 ft). The building is located in a region of high seismicity and six walls with cross section of 3.65 × 0.3 m (12 × 1 ft) have been selected to provide lateral load resistance. Eqs. (10) and (11) are used to evaluate whether special transverse reinforcement is required for the walls. The ratio of wall area to floor plan area is 0.0144 and a story height of 3.65 m (12 ft) is used. The gravity loads are based on a unit floor dead and live weight of 7.2 kPa (150 psf) and 1.9 kPa (40 psf), respectively. For h_w/l_w = 5 and p = 0.0144, use of (10) results in $\phi_u l_w$ = 0.0154. The computed gravity load at the base of the wall [assuming a tributary area of 70 m² (750 ft²)] and load factors of 1.05 for dead load and 1.28 for live load is 3.0 MN (670 kips) ($0.10 A_w f'_c$, with f'_c = 27.5 MPa (4 ksi), including a live load reduction of 60%). Assuming the walls are symmetrically reinforced, use of (11) results in $\varepsilon_{c,\max}$ = 0.0028 [for f_y = 413 MPa (60 ksi), f'_c = 27.5 MPa (4 ksi), α = 1.25); therefore, special transverse reinforcement is not required.

Based on this simple application, it is apparent that use of the proposed analytical approach does not require substantial computational effort (although the equations appear to be daunting, the terms used in the equation are relatively simple to determine), nor is it cumbersome. Preliminary design of buildings in regions of low to moderate seismic regions requires the modification of (10), which can be accomplished with readily available information in UBC-91 (*Uniform* 1991) (equivalent code spectra with R_w = 1).

Application 3: CSMIP Building 356

California Strong Motion Instrumentation Program (CSMIP) Building 356, located in San Jose, Calif., was designed and constructed in 1972. The

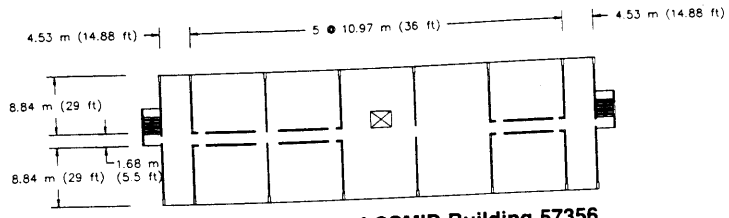

FIG. 13. Plan View of CSMIP Building 57356

building is 29 m (95 ft) high [4.1 m (13.5 ft) first story and nine stories at 2.75 m (9 ft)] with a typical floor mass of 10.7 MN (2,400 kips). The primary lateral load resisting system consists of structural walls coupled by floor slabs. A typical floor plan of the building is shown in Fig. 13. The ratio of wall area to floor plan area is 0.028 and 0.008 in the transverse and longitudinal directions, respectively. Additional building information and wall reinforcing details are provided by Moehle et al. (1990) and Wallace et al. (1990).

Strong-motion instrumentation was installed by the CSMIP and was operational at the time of the 1984 Morgan Hill and 1989 Loma Prieta earthquakes. The building was apparently undamaged in the low-to-moderate intensity motions resulting from the 1984 and 1989 earthquakes. Detailed studies of the recorded strong motion data have been conducted by Moehle et al. (1990) and Yan and Wallace (1993). Using measured building responses for the Loma Prieta earthquake, fundamental periods of approximately 0.5 s (transverse) and 0.8 s (longitudinal) were determined for the two principal directions of the building (Yan and Wallace 1993). The expected building performance based on current code requirements (*Uniform* 1991) and the approach proposed within the present paper are considered in the following sections.

UBC-91 Evaluation:

Provisions specified in UBC-91 (*Uniform* 1991) are used to determine whether the building complies with current U.S. building code requirements for regions of high seismic risk. For noncompliance, the ability of the code to provide insight into building performance is reviewed. Based on UBC-91 Eq. 34-3 (*Uniform* 1991), a period of 0.61 s is computed for each of the principal directions of the building. A code specified (factored) base shear of $0.20W$, where W is the total seismic dead load, is computed for each direction of the building based on the following coefficients: $Z = 0.4$, $S = 1.2$, $R_w = 6$. The moment resisted by the shear walls is computed by distributing the base shear over the height of the building such that the resultant lateral force acts at two-thirds of the building height from the base, and assuming that the shear walls resist all the lateral force.

The extreme fiber normal stresses for the walls, computed based on the wall moment, tributary gravity loads, and assuming a gross-concrete section inertia, are 12.1 and 33.8 MPa (1.75 and 4.90 ksi) for the transverse and longitudinal directions, respectively. Current U.S. code requirements dictate the use of well confined boundary elements if the extreme fiber stress exceeds $0.2f'_c$, or 4.1 MPa (0.6 ksi), given a concrete compressive strength of 20.7 MPa (3 ksi) for the walls. Therefore, current U.S. code requirements indicate that the walls are inadequately detailed. Even if the actual concrete strength is twice the specified value of 3 ksi, current code procedures would still dictate the use of boundary elements. However, it seems unreasonable

that well-confined boundary elements should be required where such a large number of walls are used. In addition, buildings with similar ratios of wall area to floor plan area constructed in Chile and subjected to strong ground motions during the March 3, 1985 earthquake indicated very good performance (Wallace and Moehle 1993).

Proposed Approach

To evaluate the required wall details based on the procedure outlined in the present paper, periods for the building were computed using (4). Based on the estimated gravity load [$w = 8.4$ kPa (175 psf) and the concrete materials [$E_c = 21{,}500$ MPa (3,125 ksi), periods of 0.6 ($h_w/l_w = 3.3$, $p = 0.028$) and 0.9 s ($h_w/l_w = 3.4$, $p = 0.008$) were computed for the transverse and longitudinal directions, respectively. It is noted that the computed periods agree reasonably well with the measured periods noted previously, and that the use of the computed periods provides a conservative estimate of required details.

The extreme fiber compression strain and the depth of the compression zone are computed using (11) given the following information: (1) In the transverse direction, $\rho = 0.0026$, $f_y = 413$ MPa (60 ksi); $\rho' = 0.001$, $f'_y = 413$ MPa (60 ksi); $\rho'' = 0.0025$, $f''_y = 275$ MPa (40 ksi); $P/A_w f'_c = 0.20$, $f'_c = 20.7$ MPa (3 ksi); $h_w/l_w = 3.3$; (2) In the longitudinal direction, $\rho = 0.0084$, $f_y = 413$ MPa (60 ksi); $\rho' = 0.0084$, $f'_y = 413$ MPa (60 ksi); $\rho'' = 0.0028$, $f''_y = 27.5$ MPa (40 ksi); $P/A_w f'_c = 0.08$, $f'_c = 20.7$ MPa (3 ksi); $h_w/l_w = 3.4$.

For the transverse direction (16 walls), the computed maximum compression strain is 0.0028 and the depth of the compression zone is $0.36l_w$ (for the worst condition, i.e., the wall with maximum axial load and greatest difference between tension and compression steel reinforcing ratios). For the longitudinal direction (six walls), the computed maximum compression strain is 0.0024 and the depth of the compression zone is $0.16l_w$. The analyses indicate that, for the design spectrum implied by ($3b$), $S_d = 15T$ cm ($6T$ in.), relatively low deformation demands are placed on the walls. Therefore, no special transverse reinforcement for concrete confinement is needed. In addition, buckling of longitudinal reinforcing steel at the wall boundary would not be a problem given the low compression strains. The results are also consistent with the observed performance of similar buildings constructed in Chile (Wallace and Moehle 1989, 1993).

SUMMARY AND CONCLUSIONS

A new methodology for seismic design of reinforced concrete structural walls is presented. The approach is based on comparing directly the expected displacement capacities and demands for a building. An overview of the displacement-based approach and the expected benefits compared with current code approaches are discussed. It is concluded that a displacement-based approach allows for greater design flexibility compared with current code approaches.

Earthquake ground motions are characterized based on using elastic spectral displacement relations. A simplified approach is presented to modify an elastic displacement spectrum to estimate both elastic and inelastic building displacements. It is concluded that a linear spectral displacement relationship provides a reasonable estimate of the maximum elastic or inelastic building displacement.

The expected building displacement is related to the deformations imposed on the wall cross section using well established procedures to account for the distribution of elastic and inelastic deformations over the wall height. Wall-deformation capacity is estimated based on equilibrium requirements for rectangular, flanged, and barbell wall cross sections. The deformations imposed on the wall cross section depend on the wall reinforcing ratios, the wall axial stress, the material properties of the concrete and reinforcing steel, the wall aspect ratio and configuration, and the ratio of wall cross-sectional area to floor-plan area. The relationships developed lead directly to the calculation of the magnitude and distribution of the concrete and steel strains over the wall cross section.

Transverse reinforcement for concrete confinement and to restrain buckling of the longitudinal reinforcement for structural walls can be evaluated based on the estimated magnitude and distribution of the concrete and steel strains. For buildings with symmetrically reinforced walls and wall cross-sectional area to floor-plan area exceeding 0.01, extreme fiber strains of 0.0045 or less are expected (for wall aspect ratio of 5 or less). Therefore, it is concluded that special transverse reinforcement for concrete confinement is not necessary for a large range of building and wall configurations. Similar conclusions are reached for barbell-shaped cross sections (or walls with symmetric flanges). The analyses indicate that concrete confinement is more likely for unsymmetrically reinforced walls, or walls with higher levels of axial stress. The importance of buckling of the longitudinal reinforcing steel is evaluated using a simple approach based on the tangent modulus theory. Required transverse steel to restrain longitudinal reinforcing bar buckling can be evaluated given the computed strain distribution and an assumed steel stress-strain relationship for a given bar diameter.

Three applications were presented. The displacement-based design approach presented was found to provide results that are consistent with an experimental study of a full-scale building and the observed performance of shear wall buildings in Chile subjected to strong ground motions. In addition, the applications indicated that the analytical approach is relatively simple to apply in preliminary design and may provide a valuable tool for evaluating the vulnerability of existing construction.

ACKNOWLEDGMENTS

The work presented in this paper was supported by funds from the National Science Foundation under Grant No. BCS-9010968. The writer would like to acknowledge Jack P. Moehle at the University of California, Berkeley for his valuable input on the topic of this paper. The assistance provided by Masaya Hirosawa at Kogakuin University, Japan (formerly with the Building Research Institute of Japan), in obtaining detailed information for the tests conducted at the Building Research Institute of Japan is greatly appreciated. Opinions, findings, conclusions, and recommendations in this paper are those of the writer, and do not necessarily represent those of the sponsor or of other individuals mentioned here.

APPENDIX I. REFERENCES

"Building requirements for reinforced concrete." *ACI-318* (1989). American Concrete Institute, Detroit, Mich.

Aktan, A. E., and Bertero, V. V. (1985). "RC structural walls: seismic design for shear." *J. Struct. Engrg.*, ASCE, 111(8), 1775–1791.

Hirosawa, M., Goto, T., Hiraishi, H., and Yoshimura, M. (1981). "Full-scale experimental study on aseismic performance of medium-rise RC wall structure." *BRI Res. Paper No. 91*, Building Research Institute, Ministry of Construction, Tsukuba, Ibaraki, Japan.

Mau, S. T. (1990). "Effect of tie spacing on inelastic buckling of reinforcing bars." *ACI Struct. J.*, 87(6), 671–677.

Moehle, J. P., Wallace, J. W., and Martinez-Cruzado, J. (1990). "Implications of strong motion data for the design of reinforced concrete bearing wall buildings." *Rep. No. UCB/SEMM-90/01*, Department of Civil Engineering, Univ. of California, Berkeley, Calif.

Newmark, N. M., and Hall, W. J. (1982). "Earthquake spectra and design." *Engineering monographs on earthquake criteria, structural design, and strong motion records*, Earthquake Engineering Research Institute, El Cerrito, Calif.

Paulay, T. (1986). "The design of ductile reinforced concrete structural walls for earthquake resistance." *Earthquake Spectra*, Vol. 2(4), 783–823.

Qi, X., and Moehle, J. P. (1991). "Displacement design approach for reinforced concrete structures subjected to earthquakes." *Rep. No. UCB/EERC-91/2*, Earthquake Engineering Research Center, University of California, Berkeley, Calif.

Salmon, C. G., and Johnson, J. E. (1990). *Steel structures: design and behavior*, 3rd Ed., Harper & Row, New York, N.Y.

Shimazaki, K., and Sozen, M. A. (1984). "Seismic drift of reinforced concrete structures." *Research reports*, Hazama-Gumi, Tokyo, Japan.

"Tentative provisions for the development of seismic regulations for buildings." (1978), *ATC-03-06*, Applied Technology Council, Palo Alto, Calif.

Uniform building code. (1991). International Conference of Building Officials, Whittier, Calif.

Wallace, J. W., and Moehle, J. P. (1989). "The 3 March 1985 Chile earthquake: an evaluation of structural requirements for bearing wall buildings." *Rep. No. UCB/EERC-89/5*, Earthquake Engineering Research Center, University of California, Berkeley, Calif.

Wallace, J. W., and Moehle, J. P. (1992). "Ductility and detailing requirements of bearing wall buildings." *J. Struct. Engrg.*, ASCE, 118(6), 1625–1644.

Wallace, J. W., and Moehle, J. P. (1993). "An evaluation of ductility and detailing requirements of bearing wall buildings using data from the March 3, 1985 Chile earthquake." *Earthquake Spectra*, 9(1), 137–156.

Wallace, J. W., Moehle, J. P., and Martinez-Cruzado, J. (1990). "Implications for the design of shear wall buildings using data from recent earthquakes." *Proc., 4th U.S. Nat. Conf. on Earthquake Engrg.*, 359–368.

Yan, W., and Wallace, J. W. (1993). "Analytical studies of four shear wall buildings using data from recent California earthquakes." *Rep. No. CU/CEE-93/15*, Department of Civil and Environmental Engineering, Clarkson Univ., Potsdam, N.Y.

APPENDIX II. NOTATION

The following symbols are used in this paper:

A_f = floor plan area of building;
A_s = area of tension steel;
A'_s = area of compression steel;
A''_s = area of vertical web steel;
A_v = coefficient for effective peak acceleration according to UBC-91;
A_w = $l_w \times t_w$;
a = thickness of boundary element perpendicular to wall web;
b = length of boundary element parallel to wall web;
c = length of wall cross section in compression;
c' = length of wall cross section requiring confinement;
E_c = concrete modulus of elasticity;

E_t = tangent modulus of elasticity;
d_b = diameter of reinforcing bar;
f'_c = concrete compressive strength;
f'_s = steel stress of boundary compression steel for barbell-shaped walls;
f_y = tension steel yield stress;
f'_y = compression steel yield stress;
f''_y = vertical web steel yield stress;
g = acceleration due to gravity;
h_w = total wall height;
h_w/l_w = wall aspect ratio;
h_s = story height;
I = moment of inertia;
l_p = wall plastic hinge length;
l_w = wall length;
n = number of stories;
P = axial load;
p = ratio of wall area to floor plan area;
p_{eff} = effective ratio of wall area to floor plan area;
R_w = system ductility factor according to UBC-91 (*Uniform* 1991);
S = site coefficient for soil according to ATC-03-06 ("Tentative" 1978) or UBC-91 (*Uniform* 1991);
S_a = spectral acceleration;
S_d = spectral displacement;
s = spacing of transverse reinforcement;
T = period of structure, s;
$\bar{t}$ = average wall thickness;
t_w = wall thickness;
W = weight of building;
w = unit floor weight;
Z = seismic zone factor according to UBC-91;
α = factor to account for material overstrength;
β_1 = factor as defined by ACI-318-89 10.2.7.3 ("Building" 1989);
δ_u = lateral roof displacement at ultimate;
δ_y = lateral roof displacement at yield;
$\varepsilon_{c,max}$ = extreme fiber concrete compression strain;
θ_p = plastic hinge rotation;
ρ = tension steel reinforcing ratio;
ρ' = compression steel reinforcing ratio;
ρ'' = vertical web steel reinforcing ratio;
ϕ_u = ultimate curvature; and
ϕ_y = yield curvature.